Turkish Journal of Physics

http://journals.tubitak.gov.tr/physics/

Research Article

Turk J Phys
(2014) 38: 145 – 154

doi:10.3906/fiz-1306-9

Influence of composition on the structure and optoelectronic properties of $Pb_xIn_{25-x}Se_{75}$ thin films

Hesham Azmi ELMELEEGI[1,*], Zeinab El Sayed EL MANDOUH[1], Ahmad Abdel MOEZ[2]

[1]Electron Microscope and Thin Films Department, Physical Research Division, National Research Center (NRC), Dokki, Cairo, Egypt

[2]Solid State Physics Department, Physical Research Division, National Research Center (NRC), Dokki, Cairo, Egypt

Received: 10.06.2013 • **Accepted:** 22.10.2013 • **Published Online:** 17.01.2014 • **Printed:** 14.02.2014

Abstract: $Pb_xIn_{25-x}Se_{75}$ thin films with 2 compositions were prepared by thermal evaporation. The surface topography of these films was studied by transmission electron microscope. The optical reflectance and transmittance were studied in order to determine the optical parameters such as optical energy gap, refractive index, extinction coefficient, dielectric loss, and dielectric tangent loss for these films. A single oscillator theory equation was applied for these films in order to determine both dispersion energy and oscillating energy, and the ratio of free carrier concentration/effective mass (N/m*) was determined optically. It was found that change in the composition of these films affects strongly all their optical and dielectric results.

Key words: Thin films, structure, optical properties, dielectric loss, optical conductivity, optical switching

1. Introduction

The chalcogenide semiconductors have attracted the attention of many scientists due to their good physical properties. From these compounds, lead chalcogenides narrow band gap semiconductors and their ternary compounds have attracted much attention because of their important applications as infrared detectors, photo resistors [1], lasers, solar cells [2], optoelectronic devices, thermoelectric devices, and more recently as infrared emitters and solar control coatings [2–6], high efficiency fiber amplifiers [7], and thermoelectric and photovoltaic devices [8]. As a result of their narrow band gap, lead chalcogenides and their alloys can be used as sensitive detectors for mid infrared [9]. Pattanaik et al. [10] stated that the compositional dependence of optical E_g of $Pb_xIn_{25-x}Se_{75}$ has been interpreted in terms of Kolobov's model and variation in average band energy. Deepika et al. [11] investigated the effect of changing the composition ratio of the x value on the structure and thermal analysis for $Se_{58}Ge_{42-x}Pb_x$. Hmood et al. [12] studied the effect of composition on the structure and electrical properties for ternary alloys of $PbSe_{1-x}Te_x$. They found that the electrical conductivity decreased with increasing values of x. Many other authors have investigated the effect of composition on the physical properties of $PbSe_{1-x}Te_x$ compounds [13–16]. Shamshad et al. [17] investigated the optical properties of $Se_{80}Te_{20-x}Pb_x$ with different values of x, and they found that the optical energy gap increased with increasing amounts of lead. Sushil et al. [18] investigated the influence of doping with different elements such as sulfur,

*Correspondence: eml3121@gmail.com

selenium, and tellurium on the optical, electrical, and structural properties of thin films of lead compounds. They found that the optical properties and optical band gap were affected strongly by the kind of dopant. Many authors have investigated the influence of doping on the transparent properties of lead compounds [19–21].

Majeed Khan et al. [22] studied the electrical properties of the glassy chalcogenide system Se–In–Pb. They found that there was a decrease in the density of localized states with the presence of Pb in the Se–In system. The structure and phase diagram of the Pb–In–Se system were studied [23–25]. The optical properties of the lead chalcogenide and selenide chalcogenide have been studied by many authors [26–31].

2. Experimental technique

Two compositions of the ternary compound $Pb_xIn_{25-x}Se_{75}$ were selected. The proposed compositions of the investigated system were $Pb_xIn_{25-x}Se_{75}$, where x = 1, 3. The suffix used for each element denotes its content in the system in atomic percentage. The systems of the above compositions were prepared from Pb, In, and Se pure elements with purity = 99.999%. Since some of the elements are reactive at high temperatures with oxygen, synthesis was accomplished in evacuated silica tubes $\sim 10^{-4}$ Torr that were then sealed. The inner walls of the silica tubes were coated with pure powder graphite, in order to prevent any reactions between the elements used and silica at elevated temperatures. The sealed silica tubes were heated inside a furnace at up to 1150 K and kept at this temperature for about 10 h [32]. The homogenized melt was quenched in ice-water to facilitate rapid quenching; the specimens were sealed in tubes with a small radius (about 3 mm). Thin films were prepared by vacuum thermal evaporation using an Edwards E306, and the studied films were deposited under vacuum. The structure of these films was studied using a JEOL TEM1230 (Japan) transmission electron microscope. The chemical composition of the deposited films was determined using energy dispersive X-ray spectra (EDAX) with an Oxford Instruments analytical detector with an INCA Media system attached to the JEOL TEM1230. The optical transmittance and reflectance spectra of these films were measured using a double beam spectrophotometer (JASCO Corp., V-570) with wavelength range 300–2500 nm. Optoelectronic properties were measured using a Virtins digital oscilloscope.

3. Results and discussion

3.1. Structure

To confirm the amorphous structure of thin films of $Pb_xIn_{25-x}Se_{75}$, transmission electron micrographs were obtained for the 2 compositions. Figures 1a and b, for $Pb_xIn_{25-x}Se_{75}$, x = 1, show fine grains distributed all over the film, while electron diffraction shows halos to elucidate the disorder structure. In Figures 2a and b, for $Pb_xIn_{25-x}Se_{75}$, where x = 3, the micrograph shows continuous film with no definite structure while selected area electron diffraction shows halos also confirming the amorphous structure of thin films.

3.2. Optical results

The optical transmission and reflection spectra of $Pb_xIn_{25-x}Se_{75}$ (with x values = 1 and 3) thin films are shown in Figures 3 and 4. In Figure 3, it is seen that the transmittance values are not the same; this means that the change in composition of these films leads to changes in optical properties. The behavior of reflectance for these 2 compositions also differs completely, as shown in Figure 4.

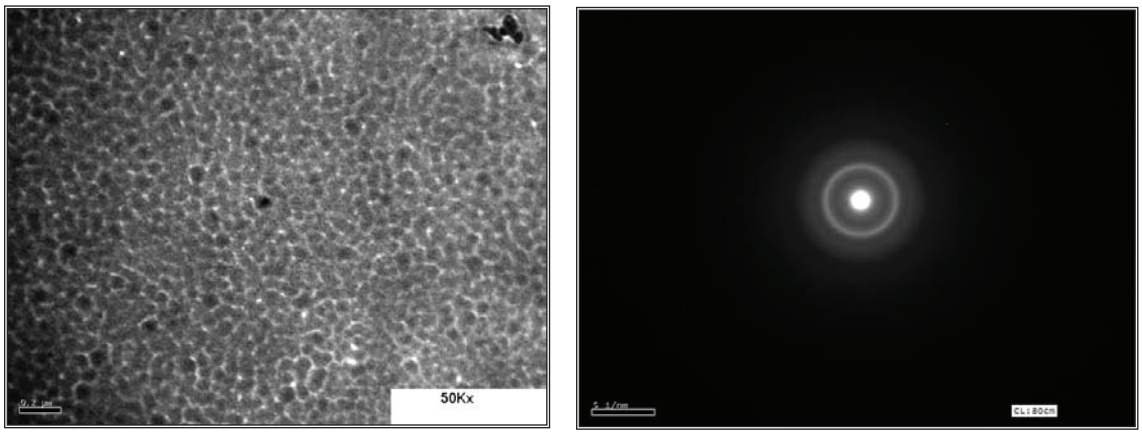

a) TEM , x = 1 b) DEM , x = 1

Figure 1. a) TEM, x = 1; b) DEM, x = 1.

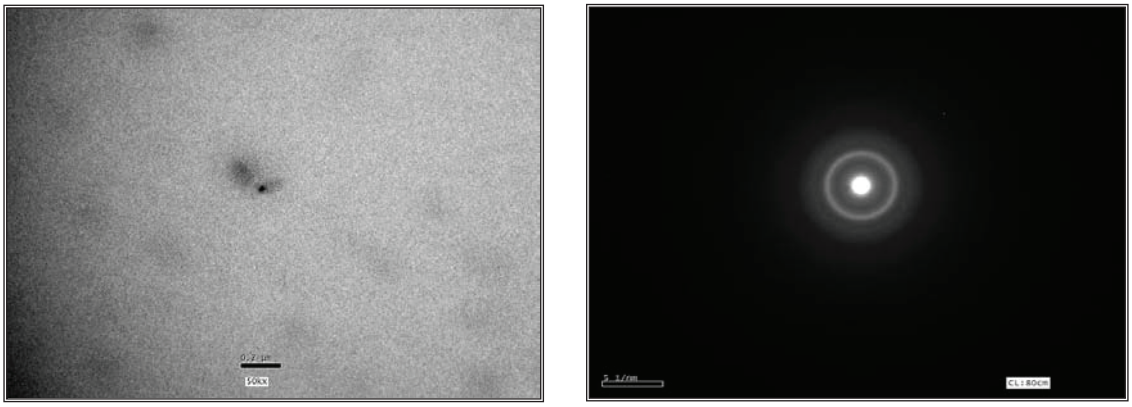

a) TEM , x = 3 b) DEM , x = 3

Figure 2. a) TEM, x = 3; b) DEM, x = 3.

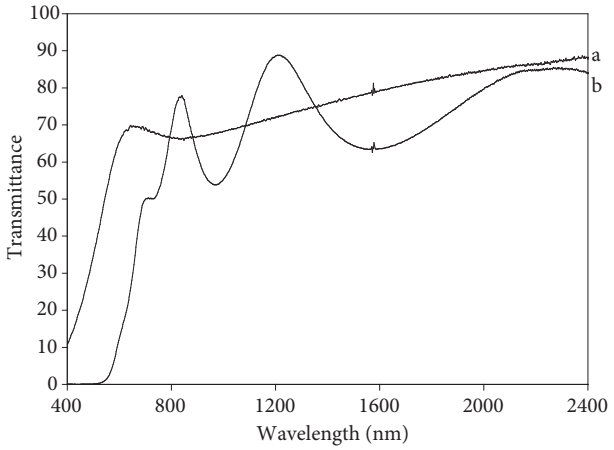

Figure 3. The transmittance spectra dependence on composition value (x) of the $Pb_xIn_{25-x}Se_{75}$ thin films for a) x = 1 and b) x = 3.

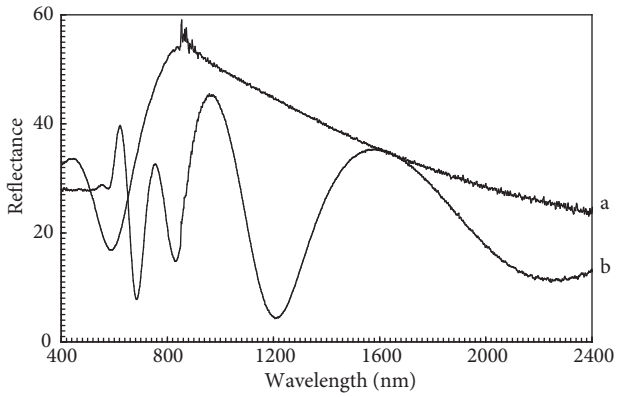

Figure 4. The reflectance spectra for $Pb_xIn_{25-x}Se_{75}$ thin films with x values a) x = 1 and b) x = 3.

The absorption coefficient (α) of these investigated films was calculated from both the transmittance and reflection spectra via the following equation [33]:

$$\alpha = \frac{1}{d}\ln\left[\frac{(1-R)^2}{T}\right], \tag{1}$$

where d is the film thickness, R is the reflectance of the studied films, and T is the transmittance of these films. The optical energy gap for these films was obtained from the absorption data using the empirical equation [34]

$$\alpha = A(h\nu - E_g)^p, \tag{2}$$

where A is a constant, E_g is the energy band gap, ν is the frequency of the incident radiation, and h is Planck's constant. The constant P takes different values depending on the kind of optical transition of these films. P = 0.5 for direct allowed transition (direct energy gap) and for indirect allowed transition P = 2.

Figure 5 shows the relation between $(\alpha h\nu)^{0.5}$ and photon energy ($h\nu$) for these films. The indirect optical energy gap for these films was determined from extrapolation of the linear part of the curves as shown in Figure 5. Figure 5 shows that the indirect optical energy gap for these investigated films has the following values: for x = 1 the energy gap = 1.5096 eV but for film with x = 3 the energy gap = 1.67 eV. This means that with increasing amount of Pb the indirect optical energy gap increases. This could be attributed to increasing electron density and electron mobility with increasing amount of Pb.

The refractive index (n) for these films was calculated using the following equation [35]:

$$n = \frac{(1+R)}{(1-R)} + \sqrt{\frac{(1+R)^2}{(1-R)^2} - (1+K)^2} \tag{3}$$

Figure 6 shows the refractive index dependence on the wavelength for thin films of 2 compositions. The behavior of the refractive index for these 2 samples is the same, but the sample with x = 1 has a greater refractive index value than the film with x = 3.

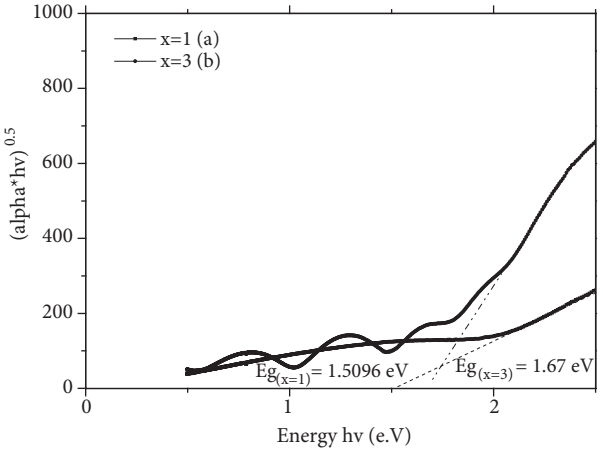

Figure 5. The relation between $(\alpha h\nu)^{0.5}$ and photon energy ($h\nu$) for $Pb_xIn_{25-x}Se_{75}$ thin films with x values a) x = 1 and b) x = 3.

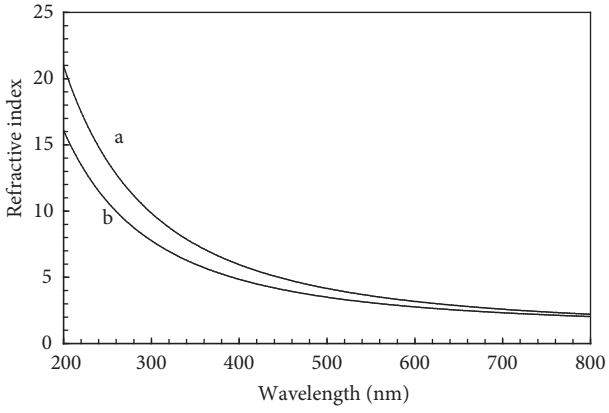

Figure 6. The refractive index (n) dependence on wavelength for Pb $_x$In$_{25-x}$Se$_{75}$ thin films with x values a) x = 1 and b) x = 3.

The single oscillator for the $Pb_xIn_{25-x}Se_{75}$ thin films with 2 values of x was determined from the relation between $(n^2-1)^{-1}$ and $(h\nu)^2$, in Figure 7, according to the Wemple–DiDomenico relationship [36]

$$n^2-1=\frac{E_0-E_d}{E_0^2-(h\nu)^2}, \tag{4}$$

where $(h\nu)$ is the photon energy, E_o is the oscillator energy, and E_d is the dispersion energy. The parameter E is a measure of the intensity of the interband optical transition, which does not affect the energy gap. The values of E_0 and E_d are obtained from the intercept on the vertical axis = (E_0/E_d) and the slope = $(E_0\ E_d)^{-1}$ resulting from Figure 7. The calculated values of E_o and E_d for these films are shown in the Table. From this table it is seen that the value of $E_o \approx 2\ E_g$ for these samples agrees with Tanaka [37].

Table.

Composition value (x)	Oscillating energy E_o (eV)	Dispersion energy E_d (eV)	N/m*	ε_L	M_{-1} (eV)	M_{-3} (eV)	Oscillator strength f $(ev)^2$	E_g e.V
1.0	4.20	5.20	5.50×10^{48}	1.80	4.70	2.00	21.84	1.509
3.0	3.60	4.70	4.10×10^{48}	1.60	4.10	1.90	16.92	1.76

The relation between $(\text{refractive index})^2$ and $(\text{wavelength})^2$ for these investigated thin films of different values of x is shown in Figure 8. The ratio of the free carrier concentration to the effective mass (N/m*) for these samples was determined optically using the following equation [38]:

$$n^2=\varepsilon_L-(\frac{e^2N}{4\pi^2c^2\varepsilon_o m^*})\lambda^2, \tag{5}$$

where ε_L is the lattice dielectric constant, ε_o is the permittivity of free space, e is the charge of electron, c is the speed of light, and (N/m^*) is the ratio of carrier concentration to its effective mass. The lattice dielectric constant ε_L can be calculated by extrapolating the linear part to intercept the n_o^2, while the slope of the obtained line in the figure is equal to the value of $(e^2.N\ /4\pi^2c^2\varepsilon_0 m^*)$. The values of (N/m*), ε_L for these films are shown in the Table.

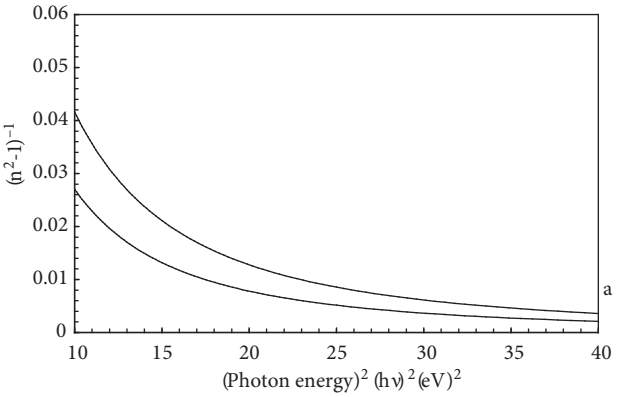

Figure 7. The relation between $(n^2-1)^{-1}$ and (photon energy)^2 for $Pb_xIn_{25-x}Se_{75}$ thin films with x values a) x = 1 and b) x = 3.

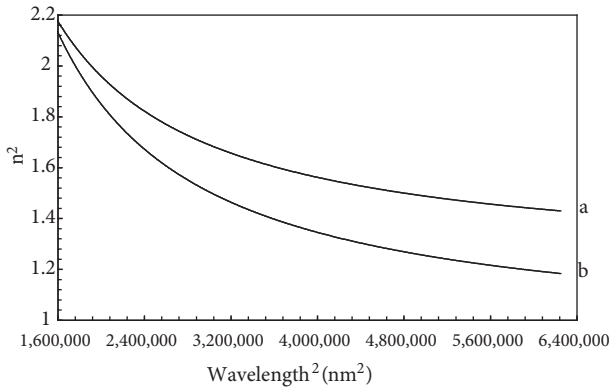

Figure 8. The relation between n^2 and $(\text{wavelength})^2$ for $Pb_xIn_{25-x}Se_{75}$ thin films with x values a) x = 1 and b) x = 3.

The determined values of E_o and E_d are related to the imaginary part of the complex dielectric constant (ε_2). The values of both M_{-1} and M_{-3} moments of the real dielectric parameter can be derived from the relation [39]

$$E_0^2 = {}^{M_{-1}}/_{M_{-3}} \tag{6}$$

$$E_d^2 = {}^{M_{-1}^3}/_{M_{-3}} \tag{7}$$

The values of both M_{-1} and M_{-3} are shown in the Table.

The oscillator strength (f) was determined optically from the values of the following equation [40]:

$$f = E_o E_d \tag{8}$$

The value of the oscillator strength is shown in the Table, where it is seen that the value of oscillator strength increases with decreasing amount of Pb of these studied films.

The dielectric parameters such as real dielectric constant (ε_1) and imaginary dielectric constant (ε_2) for these samples were determined optically using the following equations [41]:

$$\varepsilon_1 = (n^2 + k^2) \tag{9}$$

$$\varepsilon_2 = \left[(n^2 + k^2)^2 - (n^2 - k^2)^{0.5}\right] \tag{10}$$

In anisotropic media, optical constants (n, k) depend on electronic polarization of atoms, ions, or molecules of the material subjected to the electric field. The electronic polarization arises from the displacement of the negatively charged center relative to the positively charged center. As the light passes through the material, the associated field polarizes the atoms, ions, or molecules but the polarization does not respond instantly to an applied field. ε_1, which is the real part of the dielectric constant, is associated with the term that shows how much it will slow down the speed of light in the material. ε_2, which is the imaginary part of the dielectric constant, shows how a dielectric material with dielectric constant absorbs energy from the electric field due to dipole motion and so it gives information about the loss factor; indeed it is directly proportional to the loss factor. Figures 9 and 10 show the dielectric loss and dielectric tangent loss for the $Pb_xIn_{25-x}Se_{75}$ thin films

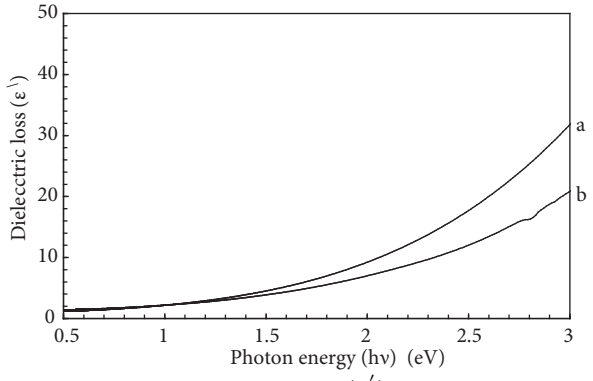

Figure 9. The dielectric loss (ε') dependence on the photon energy for $Pb_xIn_{25-x}Se_{75}$ thin films with x values a) x = 1 and b) x = 3.

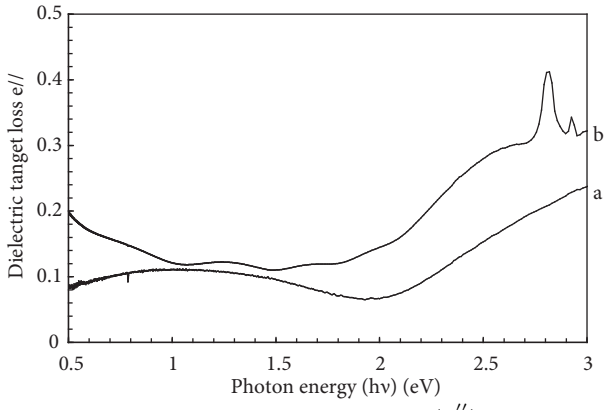

Figure 10. The dielectric tangent loss (ε'') dependence on the photon energy for $Pb_xIn_{25-x}Se_{75}$ thin films with x values a) x = 1 and b) x = 3.

with different values of x. From Figure 9 it was found that the 2 films with 2 compositions have the same behavior for the real dielectric constant but they differ at higher energies. On the other hand, in Figure 10 they had different behavior for the imaginary dielectric constant; increasing Pb leads to higher values of ε_2.

The optical conductivity (real part (σ_1) and imaginary part (σ_2)) for these investigated films was determined using the following equations [42]:

$$\sigma_1 = \frac{(\varepsilon_2 \cdot c)}{(2\lambda)} \tag{11}$$

$$\sigma_2 = \frac{(1-\varepsilon_1)\cdot c}{4\lambda} \tag{12}$$

Figures 11 and 12 show the real part (σ_1) and imaginary part (σ_2) of optical conductivity dependence on photon energy for these films. From Figures 11 and 12 it is seen that the optical conductivity increases with increasing amount of Pb, which leads to increasing mobility of free electrons in these films. The effect of absorption coefficient on optical conductivity is given in the following relation [43]:

$$\sigma = \frac{C\alpha\sqrt{\varepsilon'}}{4\pi}, \tag{13}$$

which indicates an increase in the optical conductivity with increasing absorption coefficient. The electron transitions in both the thin film and bulk material can be described using 2 important parameters, namely surface energy loss (SEL), which describe the electron transition in thin film, and volume energy loss (VEL), which describe the electron transitions in the bulk materials. The value of SEL/VEL describes the electrons transitions in this material at low and high energy [44]. The SEL of these 2 samples with different compositions was calculated and plotted as a function of photon energy as shown in Figure 13 using the following equations [45]:

$$SEL = \frac{\varepsilon_2}{(\varepsilon_1+1)^2+\varepsilon_2^2} \tag{14}$$

$$VEL = \frac{\varepsilon_2}{\varepsilon_1^2+\varepsilon_2^2} \tag{15}$$

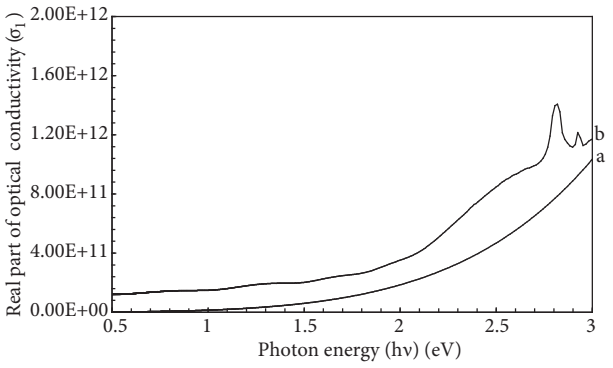

Figure 11. The real part of photo conductivity (σ_1) dependence on the photon energy for $Pb_xIn_{25-x}Se_{75}$ thin films with x values a) x = 1 and b) x = 3.

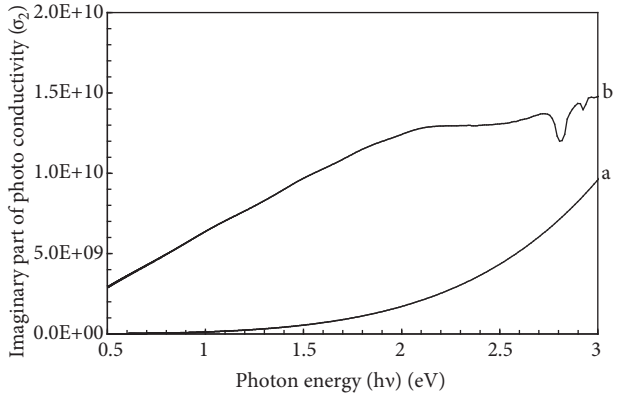

Figure 12. The imaginary part of photo conductivity (σ_2) dependence on the photon energy for $Pb_xIn_{25-x}Se_{75}$ thin films with x values a) x = 1 and b) x = 3.

Figure 13 shows the VEL/SEL dependence on photon energy. From this figure it is clear that there is an electron transition at low energy (lower than energy gap) for $Pb_xIn_{25-x}Se_{75}$ with x = 1, while for $Pb_xIn_{25-x}Se_{75}$ film with x = 3 there is no electron transition. This could be attributed the fact that there are sublevels or doping level due to the excess of In.

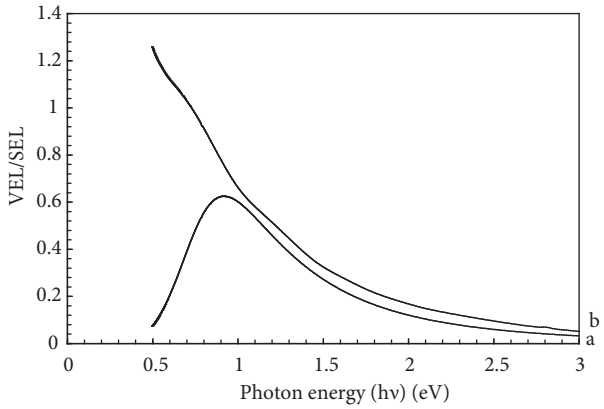

Figure 13. The relation between VEL/SEL and photon energy $Pb_xIn_{25-x}Se_{75}$ thin films with x values a) x = 1 and b) x = 3.

3.3. Optical switching

Switching of $Pb_xIn_{25-x}Se_{75}$ with x = 1 thin film observed in Figure 14a due to irradiation of sample by UV light shows 2 curves: the on-state of switching operation for the wavelength 1000 nm and the off-state for the wavelength 800 nm. Therefore, this sample is a promising candidate for optical switching.

On the other hand, for the composition $Pb_xIn_{25-x}Se_{75}$ with x = 3 (Figure 14b), no switching was observed by applying different light wavelengths of 200, 500, 800, and 1000 nm.

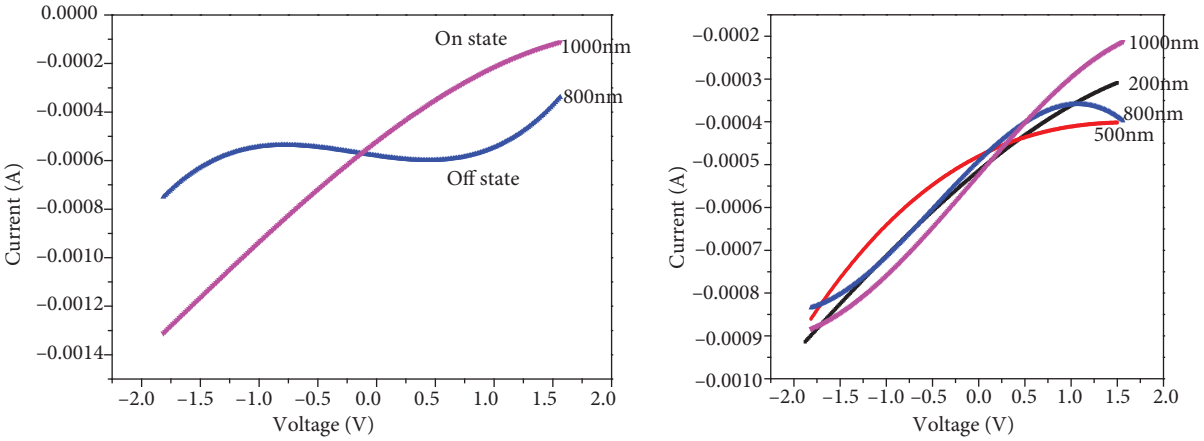

a) Switching appears x = 1.0 b) Switching doesn't exist x = 3.0

Figure 14. Relation between current vs. voltage under light exposure of variety of wavelengths. a) Switching appears x = 1.0; b) Switching does not exist x = 3.0.

Irradiation influences the structure of glassy chalcogenide materials; new defects appear, film crystallization phase transition may happen, or transition from meta-stable state to another unstable state occurs [46].

Photo-induced changes in chalcogenide glasses were observed at very small levels of light excitation as high as 10^{-6} to 10^{-2} W cm^{-2} [47]. As charge transport in amorphous materials is controlled by traps, at any moment a significant fraction of carriers is trapped. The dipole moments of the filled traps may be different from that of empty traps. As a result, the dielectric permittivity of the material becomes dependent on trapped carriers and the dependence of dielectric permittivity (ε) on time and coordinate appears. To ensure this, in the Time of Flight experiment, during the packet movement the trapped carrier density changes and hence that dependence of ε on time and coordinate is revealed. The transient dielectric constant causes an additional displacement current, which may be negative relative to the electric-field direction [48]. In a certain time interval, this additional current can dominate. As a result, the total current of the sample becomes negative. Note that: 1) the polarization current may be due both to traps distributed in the volume and to surface traps; 2) the polarization due to the volume traps alone is unable to describe the observed values and the behavior of the negative transient current. This fact shows the remarkable role of the surface traps in the mechanism of negative current generation.

4. Conclusion

High quality $Pb_xIn_{25-x}Se_{75}$ thin films were prepared with 2 values of x (x = 1 and 3). The optical parameters such as transmittance and reflectance of these films were studied. The optical indirect energy gap was calculated, which decreases with increasing amount of Pb, due to the increase in the number of free electrons and also the increased the mobility of these electrons. The dispersion and oscillating energy for these films showed that the composition value (x) of films strongly affects these results. The ratio between (N/m*) effective mass for these films was calculated optically. The optical conductivity was determined, and it showed that it increases with increasing amount of Pb. Finally, the ratio between SEL and VEL was determined optically. These results give us an excellent chance to control the optical and dielectric properties of these films by changing the composition ratio of these films' constituents.

References

[1] Chao, I. Na.; McCann, P. J.; Yuan, W. L.; Yuan, S. *Thin Solid Films* **1998**, *323*, 126–135.

[2] Meca, F. J.; Quintas, M. M.; Sanchez, F. J. R. *Sensors Actuators* **2000**, *84*, 45–52.

[3] Dashevsky, Z.; Shusterman, S.; Dariel, M. P. *J. Appl. Phys.* **2002**, *92*, 1425–1430.

[4] Ibrahim, M. M.; Saleh, S. A.; Ibrahim, E. M. M.; Abdel Hakeem, A. M. *J. Alloys Compd.* **2008**, *452*, 200–204.

[5] Ibrahim, M. M.; Ibrahim, E. M. M.; Saleh, S. A.; Abdel Hakeem, A. M. *J. Alloys Compd.* **2007**, *429*, 19–24.

[6] Ding, Q. Li.; Shao, Y. M.; Wu, J.; Yu, G.; Qian, Y. *Mater. Res. Bull.* **2003**, *38*, 539–543.

[7] Takats, V.; Nemec, P.; Csik, A.; Kokenyesi, S. *J. Phys. Chem. Solids.* **2007**, *68*, 948–952.

[8] Pattanaik, A. K.; Srinivasan, A. *J. Appl. Sci.* **2005**, *5*, 1–4.

[9] Zogg, H.; Arnold, M. *Infrared Phys. Technol.* **2007**, *49*, 183–186.

[10] Khan, S. A.; Zishan, H. K; El-Sebaii, A. A.; Al-Marzouki, F. M.; Al-Ghamdi, A. A. *Physica B.* **2010**, *405*, 3384–3390.

[11] Deepika, P.; Jain, K.; Rathore, K. S.; Saxena, N. S. *J. Non-Crystalline Solids* **2009**, *355*, 1274–1280.

[12] Hmood, A., Kadhim, A.; Abu Hassan, H. *Superlattices and Microstructures* **2012**, *51*, 825–833.

[13] Kumar, S.; Hussian, M.; Sharma, T. P.; Husian, M. *J. Phys. Chem. Solids.* **2003**, *46* 367–376.

[14] Kumar, S.; Majeed Khan, M. A.; Shamshad, A. K.; Husain, M. *Opt. Mater.* **2004**, *25*, 25–32.

[15] Xiaochuan, X.; Lidong, C.; Chunfen, W.; Qin, Y.; Chude, F. *J. Solid State Chem.* **2005**, *178*, 2163–2166.

[16] Li, J. Q.; Li, S. P.; Wang, Q. B.; Wang, L.; Liu, F. S.; Ao, W. Q. *J. Alloys Compd.* **2011**, *509*, 4516–4519.

[17] Shamshad, A. K.; Zulfequar, M.; Husain, M. *Current Applied Physics* **2005**, *5*, 583–587.

[18] Sushil, K.; Bhajan, L.; Aghamkar, P.; Husain, M. *J. Alloys Compd.* **2009**, *488*, 334–338.

[19] Trajic, J.; Golubovic, A.; Romcevic, M.; Romcevic, N.; Nicolic, S.; Nikiforov, V. *J. Serb. Chem. Soc.* **2007**, *72*, 55–62.

[20] Hankare, P. P.; Delekar, S. D.; Chate, P. A.; Sabane, S. D.; Daradkar, K. M.; Bhuse, V. M. *Semicond. Sci. Technol.* **2005**, *20*, 257–264.

[21] Samoylov, A. M.; Sharov, M. K.; Buchnev, S. A.; Khoviv, A. M.; Dolgopolova, E. A. *Journal of Crystal Growth* **2002**, *240*, 340–346.

[22] Majeed Khan, M. A.; Zulfequar, M.; Kumar, A.; Husain, M. *Materials Chemistry and Physics* **2004**, *87*, 179–183.

[23] Recorda, M. C.; Ilyenko, S.; Daouchi, B.; Tedenac, J. C. *J. Alloys Compd.* **2001**, *316*, 239–244.

[24] Daouchi, B.; Record, M. C.; Tedenac, J. C. *J. Alloys Compd.* **2000**, *296*, 229–232.

[25] Lin, J. C.; Sharma, R. C.; Chang, Y. A. *J. Phase Equilibria* **1996**, *17*, 253–260.

[26] Wang, H.; Zhang, X.; Yang, G.; Xu, Y.; Ma, H.; Adam, J. L.; Gu, Z.; Chen, G. *Ceramics International* **2009**, *35*, 83–86.

[27] Bhardwaj, A.; Varadarajan, E.; Srivastava, P.; Sehgal, H. K. *Solid State Communications* **2008**, *146*, 53–56.

[28] Badr, Y.; Mahmoud, M. A. *Physica B: Condensed Matter.* **2007**, *388*, 134–138.

[29] Ateş, A.; Gürbulak, B.; Yıldırım, M.; Doğan, S. *Physica E: Low-dimensional Systems and Nanostructures* **2003**, *16*, 274–279.

[30] Salem, A. M.; El-Gendy, Y. A.; El-Sayad, E. A. *Physica B: Condensed Matter.* **2009**, *404*, 2425–2430.

[31] Zishan, S. K.; Khan, H.; Majeed Khan, M. A.; Husain, M. *Current Applied Physics* **2005**, *5*, 561–566.

[32] Sukla, R. K.; Swarup, S.; Agnihotri, A. K.; Nigam, A. N.; Kumar, A. *Phil. Mag. Lett.* **1991**, *63*, 165–171.

[33] Fadel, M.; Fayek, S. A.; Abou-Helal, M. O., Ibrahium, M. M.; Shakra, A. M. *J. Alloys Compd.* **2009**, *485*, 604–609.

[34] Aranda, J.; Morenza, J. L.; Esteve, J.; Codina, J. M. *Thin Solid Films* **1984**, *120*, 23–30.

[35] Singh, D.; Kumar, S.; Thangaraj, R. *J. Non-Cryst. Sol.* **2012**, *358*, 2826–2834.

[36] Torris, J.; Cisneros, J. I.; Gordillo, G.; Alvarez, F. *Thin Solid Films* **1996**, *289*, 238–241.

[37] Tanaka, K. *Thin Solid Films* **1980**, *66*, 271–279.

[38] Kumar, G. A.; Thomas, J.; George, N.; Kumar, B. A.; Radhkrisnam, P.; Nempoori, V. P. N.; Vallobhan, C. P. G. *Phys. Chem. Glasses* **2000**, *41*, 89–93.

[39] Farid, A. M.; El-Zawawi, I. K.; Ammara, A. H. *Vacuum* **2012**, *86*, 1255–1261.

[40] Wemple, S. H.; DiDomenico, M. Jr. *Phys. Rev. Lett.* **1969**, *23*, 1156–1160.

[41] Djurišić, A. B.; Li, E. H. *Optics Communications* **1998**, *157*, 72–76.

[42] Ammar, A. H.; Frid, A. M.; Sayam, M. A. M. *Vacuum* **2002**, *66*, 27–38.

[43] Kireev P. S. Semiconductor Physics Mir Publishers. **1974**, 523.

[44] Tan, G. L.; DeNoyer, L. K.; French, R. H.; Guittet, M. J.; Gautier-Soyer, M. *Materials Science and Engineering* **2000**, *294–296*, 867–870

[45] Ammar, A. H.; El-Sayed, B. A.; El-Sayad, E. A. *J. Mat. Sci.* **2002**, *37*, 3255–3260.

[46] Popescu, M.; Andriesh, A.; Ciumash, V.; Iovu, M.; Tsiuleanu, D.; Shutov, S.; Fizica Sticlelor Chalcogenidce (Physics of Chalcogenide Glasses) Editura Stiintifica, Bucaresti I.E.A. Stiinta Press, Chisinan in Romania, 1996.

[47] Andriesh, A. M.; Culeac, I. P.; Loghin, V. M. *Journal of Non-Crystalline Solids* **1989**, *114*, 136–138.

[48] Fairman, R.; Ushkov, B. *Semiconducting Chalcogenide Glasses* II, vol. 79, Elsevier: New York, NY, USA, 2004.